Local migration quantification method for scratch assays

Ana Victoria Ponce Bobadilla*[1,2], Jazmine Arévalo[3], Eduard Sarró[3], Helen M Byrne[4], Philip K Maini[4], Thomas Carraro[1,2], Simone Balocco[5,6], Anna Meseguer[3,7,8], and Tomás Alarcón †[9,10,11,12]

[1] Institute for Applied Mathematics, Heidelberg University, 69120 Heidelberg, Germany
[2]Interdisciplinary Center for Scientific Computing (IWR), Heidelberg University, 69120 Heidelberg, Germany
[3]Renal Physiopathology Group, CIBBIM-Nanomedicine, Vall d'Hebron Research Institute, Barcelona, Spain
[4]Wolfson Centre for Mathematical Biology, Mathematical Institute, University of Oxford, Oxford OX2 6GG, UK
[5]Dept. Matematics and Informatics, University of Barcelona, Gran Via 585, 08007 Barcelona, Spain
[6]Computer Vision Center, 08193 Bellaterra, Spain
[7] Departament de Bioquímica i Biologia Molecular, Unitat de Bioquímica de Medicina, Universitat Autònoma de Barcelona, Bellaterra; Spain
[8] Red de Investigación Renal (REDINREN), Instituto Carlos III-FEDER, Madrid, Spain
[9] ICREA, Pg. Lluís Companys 23, 08010 Barcelona, Spain
[10] Centre de Recerca Matemàtica, Edifici C, Campus de Bellaterra, 08193 Bellaterra (Barcelona), Spain
[11]Departament de Matemàtiques, Universitat Autònoma de Barcelona, 08193 Bellaterra (Barcelona), Spain
[12] Barcelona Graduate School of Mathematics (BGSMath), Barcelona, Spain

Abstract

The scratch assay is a standard in vitro technique for studying the underlying mechanisms in cell migration and assessing compounds for clinical use. Current quantification methods of scratch assays deal poorly with irregular cell-free areas and crooked leading edges which are features typically present in the experimental data. We introduce a new migration quantification method that allows us to analyse low quality experimental data and perform a better statistical classification of migration rates than two of the current standard quantification methods. By performing a classification test on in silico data, we show that the method exhibits significantly lower statistical errors compared to the standard methods. Considering in vitro data, our method outperforms the standard methods by detecting differences in the migration rates between different cell groups that the other methods could not detect. Application of this new method will enable the quantification of migration rates of in vitro scratch assay data previously unsuitable for analysis.

Keywords— scratch assays, migration quantification methods, migration rates, statistical classification

1 Background

Cell migration plays a fundamental role in developing and maintaining the organization of multicellular organisms, while aberrant cell migration is found in many pathological disorders like cancer and atherosclerosis [1, 2]. In vitro assays are central to the study of cell migration since they allow us to quantify the cell migratory capacity under controlled experimental conditions [3, 4]. The scratch or wound healing assay is the method of choice for studying cell migration due to the low cost and simplicity of its experimental design [3, 5]. A scratch assay involves: growing a cell monolayer to confluence in a multiwell assay plate; creating a "wound" -a cell-free zone in the monolayer- into which cells can migrate; and monitoring the recolonisation of the scratched region to quantify the cell motility [5] (see Figure 1). This experimental technique is commonly used to understand the molecular mechanisms that affect cell migration [6, 7] and to identify pharmaceutical compounds that can modulate cell migration and consequently drive treatment therapies [8]. Given the key role of scratch assays in biomedical research, it is important to develop robust quantification methods that accurately measure and compare migration rates of different scratch assays.

Multiple quantification methods are used to assess collective cell migration in scratch assays [11]. The most common ones focus on the wound size evolution [4, 12]. Such methods use a number of metrics to quantify

*anavictoria.ponce@iwr.uni-heidelberg.de
†Talarcon@crm.cat

migration, including the percentage difference in the wound sizes at different time points [7, 13], the wound size at specific time points [14], and the slope of a linear approximation to the evolution of the wound area [15] among others. A major disadvantage of current methods is that they do not perform well when the two borders of the scratch are not perfectly straight, which is a feature typically present in the experimental data [15, 16]. The lack of a reproducible wounding procedure results in non-uniform cell-free areas with irregular leading edges, as can be seen in Figure 1. Furthermore, migration rate measurements have been shown to be sensitive to the initial degree of confluence [17] and the initial geometry of the wound [18]. Current quantification methods require high quality experimental data which are difficult to obtain; therefore, frequently the experimental data are discarded or need to be produced again.

Another issue with current quantification methods is that most of them consider time-specific measurements to determine differences in migration rates of wound healing samples. Typically, a time point in the course of the experiment is considered in which the wound area or width of the samples are measured. Then, statistical tests are performed on these measurements with the purpose of detecting significant differences [4]. The time points of comparison are not standardized and vary across studies [7, 19, 20]. The problem is that the choice of time points can affect the comparison, making the results uncertain.

In this work, we introduce a new quantification method that tackles these issues and can be used to analyse lower quality experimental data. Irregular leading edges are accounted for by approximating the front by a piecewise constant function, which is constant over windows with a fixed size, w^*. We assume that within each window, the contour moves with constant speed in the perpendicular direction until the two leading edges meet. The migration in the scratch assay is characterized by a series of linear approximations to the interface evolution in these windows.

The paper is organized as follows: in Section 2.1 we describe our experimental system and in Section 2.2 we present the agent-based model that we use to simulate the in vitro process. In Section 2.4 we introduce the new migration quantification method for scratch assays and describe the two quantification methods to which we compare it: the *percentage wound area method* which is widely used and the *closure rate method*, introduced by [15]. In Section 3.1.1, we investigate how the velocity distribution, determined by our quantification method, is affected by cell motility and proliferation. In Section 3.1.2 we show that the method correctly classifies cells with different motility and proliferation parameters. In Section 3.1.3 we show the statistical comparision against the other methods. In Section 3.2.3, we present the results of applying the three methods to a experimental data set. Finally in Section 4, we discuss our results and present our conclusions.

2 System and methods

2.1 Cell culture and wound healing assay

Six site-specific mutations in a latent transcription factor that regulates downstream genes involved in essential biological processes, including migration, were generated. Mutants S1, S2, S3, S4, S5 and S6 were then transduced into a human renal carcinoma cell line, 769-P (ATCC CRL-1933), through lentiviral particles. The 769-P mutants were cultured in Dulbecco's Modified Eagle's Medium (DMEM) (#42430, Gibco) supplemented with 10% of fetal bovine serum (FBS) (#10270, Gibco), 1% of sodium pyruvate solution 100 mM (#03-042-1B, Biological Industries) and 1% of antibiotic-antimycotic solution 100X (#15240, Gibco). Cells were maintained at 37°C in 5% CO_2.

For the wound healing assay, the 769-P mutants (S1-S6) were seeded at 0.025×10^6 cells per well in a 2 well silicone insert with a defined cell-free gap (Ibidi #81176, Germany), incubated and allowed to grow for 48 hr. Once the cells reached 100% confluence, the culture insert was removed and the area that remained clear of cells was quantified for 24 hr using the Live Cell-R Station (Olympus). Digital images were obtained every 30 minutes.

Data consisted of 24 wound healing assays: four replicates for each of the six groups (S1-S6). Each assay consisted of 48 images. The imaged region size was 500×500 $[\mu m]^2$.

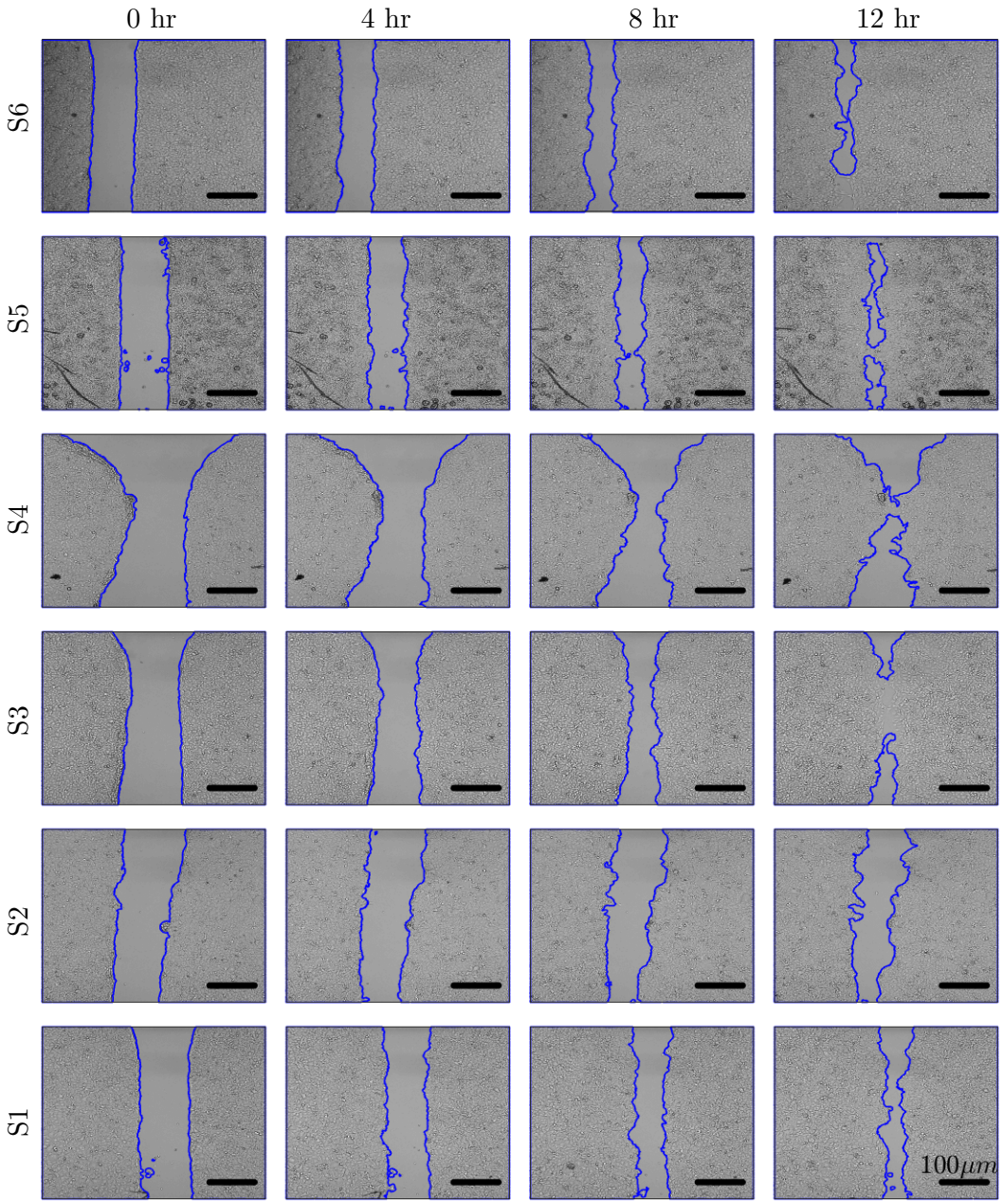

Figure 1: The evolution of a representative scratch from each of the six cell groups (S1-S6) from our experimental data is plotted at time 0 hr, 4 hr, 8 hr and 12 hr. In each image, the leading edges have been detected by applying the segmentation algorithm. The detected interfaces/cell fronts are plotted in blue.

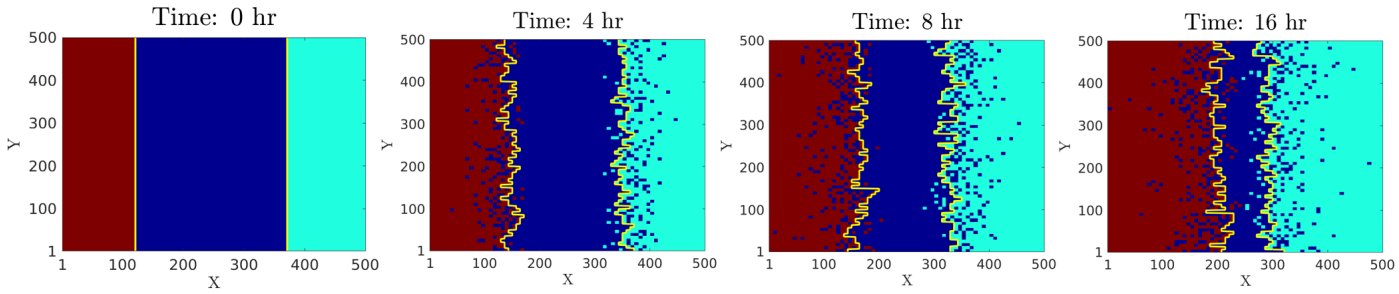

Figure 2: Evolution of an agent-based simulation. We considered an idealised initial condition and fixed the motility and proliferation parameters so that $p_m = 0.3$ and $p_p = 0.01$, respectively. The recolonisation of the wounded region is shown at times $t = 0, 4, 8$ and 16 hr. The two cell monolayers are plotted with different colours (red and turquoise), while the area devoid of cells is coloured blue. The leading edges detected by the segmentation algorithm are plotted in yellow.

2.2 Agent-based model of the scratch assay

We consider an agent-based model that has been previously used to simulate in vitro cell cultures [21, 22, 23]. The simulation domain is a two-dimensional square lattice, with the same dimensions as the experimental images: $[0, D] \times [0, D]$ where $D = 500$ μm. The lattice spacing, Δ, which is interpreted as the average cell diameter, is set to 10 μm unless otherwise specified.

In this model each agent can either proliferate or move within the simulation domain. We consider an end time of $T = 24$ hr and an update time of $\tau = 0.1$ hr. We include crowding effects by assuming that each lattice site is occupied by at most one cell. A cell with centre at (x, y) is said to be at (x, y). Zero flux boundary conditions are imposed. At each update time, agents can move and/or proliferate with motility and proliferation probabilities p_m and p_p respectively. Since typical estimates of the cell doubling time are approximately 15-30 h [24, 25], whereas the time required for a cell to move a distance equal to its diameter is of 10 min [26], we consider the motility and proliferation probabilities in the ranges $p_m \in [0, 1]$ and $p_p \in [0, 0.01]$, respectively. The simulation algorithm and typical parameters values are presented in the Supplementary Material Section 1. In Figure 2 we plot the evolution of a typical realisation of the agent-based model simulation for which the motility and proliferation parameters are given by $p_m = 0.3$ and $p_p = 0.01$, respectively.

2.3 Automatic contour segmentation

The leading edges of the cell monolayers from the experimental images are detected by applying a segmentation algorithm based on the Growcut method [27]. The method is a robust technique, already employed in several computer vision applications, that performs a binary image segmentation.

The Growcut algorithm requires the initial specification of a subset of pixels from each type of region: cell monolayer and unoccupied space; these pixels are referred to as *seeds*. The seeds should be located far from the leading edges, where all the pixels of such an area belong to one of the two classes. The algorithm evolves as follows: at each iteration, the pixels surrounding the initial seeds are assigned to one class or the other, adjusting the size of each region. The classification depends on the similarity of the pixel intensity with respect to the pixel intensity of the seeds.

In our implementation, the seeds are chosen as follows: for the cell region, the Canny and Roberts edge contour methods [28, 29] are used to select the pixels with the highest variability, corresponding to the cell contours. For the background region, the seeds are set in areas having a low variability, defined as areas in which the pixel intensity has a standard deviation less than 500.

After applying the detection algorithm to each image, we have a record of the positions of the left and the right interfaces at each time where the image was taken. At each vertical position, the interface is consider to be the closest pixel to the wound.

2.4 Migration quantification methods

We first introduce the two established quantification methods for scratch assays. Then, we introduce a new method that quantifies the x-component of the velocity of the leading edge of the cell monolayer.

2.4.1 Percentage wound area method

The most common quantification method, which we refer to as the *area method*, assesses the migration in an indirect manner. In the course of the experiment, the wound area percentage, $\hat{A}(t)$, is tracked:

$$\hat{A}(t) := \frac{A(t)}{A(0)} \times 100\%$$

where $A(t)$ is the wound area at time t and $A(0)$ is the initial area. The migration rate is then indirectly evaluated as the percentage wound area at a specific time point.

2.4.2 Closure rate method

[15] proposed a method for quantifying cell migration with respect to the slope of a linear approximation to the evolution of the wound area. We refer to this method as the *closure rate method*. The evolution of the wound area $A(t)$ is first approximated by a linear function:

$$A(t) \approx m \times t + b \tag{1}$$

where m and b are real scalars. The wound area is assumed to be the length of the field-of-view (l) times the width of the gap ($W(t)$). Since l is constant during the course of the experiment, Equation (1) becomes:

$$\frac{dA}{dt} \approx l \times \frac{dW}{dt}. \tag{2}$$

The migration rate, C_r, is defined to be half of the width closure rate

$$C_r := \frac{1}{2}\frac{dW}{dt}. \tag{3}$$

From Equations (2) and (3), we have

$$C_r = \frac{|m|}{2 \times l}. \tag{4}$$

2.5 Proposed quantification method: velocity method

We propose a new strategy for quantifying front migration in a scratch assay by a set of representative velocities. We denote by $t_0, \ldots, t_N$, the times at which data are collected. Let $X \times Y$ represent the square domain of the processed image, $X = Y = \{1, \ldots, D\}$ where D is the number of pixels. For each $j \in Y = \{1, \ldots, D\}$, we denote the interface position in the horizontal direction, at the $j-$th vertical position and at time point t_n, as $i_j(t_n)$ where $1 \leq i_j \leq D$. See Figure 3 A for a schematic representation.

To determine the velocities, we perform a linear approximation to the front evolution with respect to a window size w. The linear approximation is defined in two steps:

1. First, the front position is approximated with respect to the window size, w. Y is divided into $M = D/w$ Y_s segments of length w. The front position in each segment Y_s is approximated by its mean position,

$$\hat{i}_s(t_n) = \langle i_j(t_n) \rangle_{i_j \in Y_s}. \tag{5}$$

This procedure is illustrated in Figure 3 B).

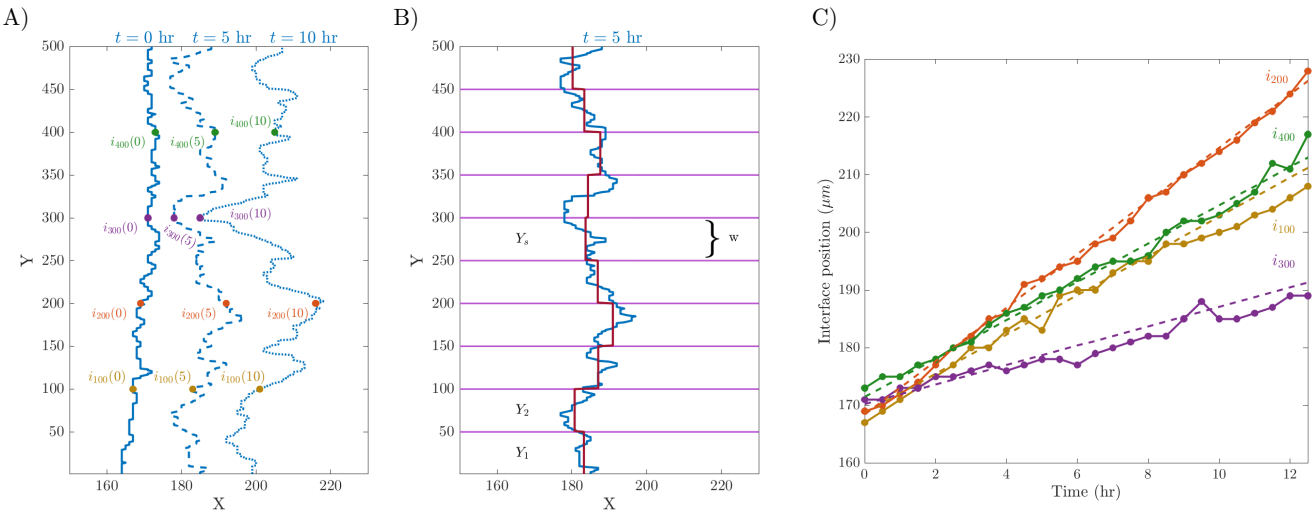

Left front evolution

Front approximation with respect to window size w

$$\hat{i}_s(t_n) = \langle i_j(t_n) \rangle_{p_j \in Y_s}$$

Linear approximation for the front evolution

$$\hat{i}_s(t_n) \approx m_s t_n + b_s$$

Figure 3: Linear approximation of the front evolution with respect to window size w. A) To introduce the notation, the left front position at times $t = 0, 5$, and 10 hr are plotted in blue. The solid line corresponds to $t = 0$ hr, the dashed line to 5 hr and the dotted line to 10 hr. The front position at the 100, 200, 300 and 400 y-coordinates for these times is plotted in different colours: yellow, orange, purple and green, respectively. B) The left front at $t = 5$ hr is approximated by a window size w. Y is partitioned into Y_s segments each with length w. A magenta horizontal line delimits each segment. The front position is plotted in blue and the approximated front position, taken as an average over each Y_s, is plotted in red. C) The interface evolution at the 100, 200, 300 and 400 y-coordinates and the linear approximation with respect to the window size $w = 12$ are plotted in full lines and dashed lines, respectively. The window size $w = 12$ is the window size that maximizes the objective function (7).

2. The front evolution along each window is approximated by a linear regression

$$\hat{i}_s(t_n) \approx m_s t_n + b_s. \tag{6}$$

In Figure 3 C) the solid lines represent the front evolution at selected y-coordinates; the dashed lines represent the corresponding linear approximations for a window of size $w = 16$.

Performing this approximation for the left and right interfaces, we obtain a set of velocities $\{|m_s|\}_{s=1}^{2M}$ which we refer to as the windowed velocities for window size w.

Given a window size w, we expect the left and right windowed velocity distributions to be similar, since both fronts were initially part of the same cell monolayer. However, for window sizes smaller than the average cell size, the distributions are significantly different. This is because the scale on which the velocities are approximated is much smaller than the cell size scale: the individual velocity of each cell at the front is counted multiple times and its value is over represented, producing a bias in the overall windowed velocity distribution. In practice, we choose a window size for which the left and right windowed velocity distributions are similar.

The key step of our method is to determine the optimal window size to perform the linear approximation (6). We use two criteria to select the optimal window size, w^*: (i) fitness of the approximation, and (ii) similarity of the left and right windowed velocity distributions. We consider an objective function, $F(w)$, that allows us to find the optimal window size with respect to these two criteria. The objective function has three terms:

$$F(w) = Fit_{resid}(w) + Fit_{Rsquared}(w) + Fit_{KS_{distance}}(w). \tag{7}$$

- $Fit_{resid}(w)$ measures the discrepancy between the interface evolution and the linear approximation (Equation (6)).
- $Fit_{Rsquared}(w)$ considers the coefficient of determination, R^2, which describes how well the evolution variance is explained by the linear approximation [30].
- $Fit_{KS_{distance}}(w)$ is a distance function derived from the Kolmogorov-Smirnov statistic for the two-sample Kolmogorov-Smirnov (K-S) test [30] that calculates the distance between the left and right front windowed velocity distributions.

The terms are scaled such that the window size that maximises the objective function gives the best fit and has the left and right velocity distributions which are closest to each other. Detailed information about the objective function can be found in Supplementary Material Section 2.

The steps used to determine the set of representative velocities are summarized in Algorithm 1.

Algorithm 1 : Velocity quantification method

1: Determination of the optimal window size for the linear approximation using the objective function (7)

$$w^* = \max_{1 \le w \le D} F(w) \tag{8}$$

where $F(w)$ is given by equation (7).

2: Linear approximation with respect to the window size w^* for the evolution of the left and right interfaces,

$$\hat{i}_s(t_n) \approx m_s t_n + b_s$$

where $\hat{i}_s(t_n) = \langle i_j(t_n) \rangle_{i_j \in Y_s}$, $Y = \bigcup_{s=1}^{M} Y_s$ in which $|Y_s| = w^*$ and $M = D/w^*$.

Output: $\{|m_s|\}_{s=1}^{2M}$ is the representative set of velocities that quantify the migration in the scratch assay.

2.6 Classification test

In order to assess the performance of the three quantification methods in a controlled way, we use the agent-based model to generate in silico scratch assays. In particular, we compare the ability of the different methods

to distinguish between cell populations with different proliferation and motility parameters. We consider the following classification test:

1. We fix a focal parameter combination $\hat{P} = (p_{\hat{m}}, p_{\hat{p}}) \in [0,1] \times [0, 0.01]$ and run n simulations of the agent-based model using these parameter values.

2. We decompose the parameter space of motility and proliferation probabilities $[0,1] \times [0, 0.01]$ into a regular 11×11 grid with 121 parameter pairs (p_m, p_p). For each parameter combination, we run n simulations of the agent-based model.

3. We calculate the cell migration rate in all simulations using the three quantification methods. The migration measurements are windowed velocities, closure rates or areas at specific time points, depending on the quantification method.

4. For each quantification method, we determine whether the migration measurements of each sampled parameter combination (p_m, p_p) are statistically significantly different from those for the focal parameter pair $\hat{P}$. We perform two tests: the two-sample Kolmogorov-Smirnov test and the unpaired two-sample t-test, which we refer as the K-S test and t-test, respectively. We fix a p-value < 0.05 to define statistical significance.

We consider a K-S test and a t-test to test for differences at the distribution level and in the mean. We test our data for normality and in case the migration measurements are not normally distributed, we consider a Wilcoxon rank-sum test. We account for stochasticity of the agent-based model by repeating this test for 20 times and analyse the mean and variance of the classification results.

When applying the classification test to the velocity method, we consider a global optimal window size for determining the windowed velocities of the simulations. In this way, we obtain the same number of windowed velocities for each simulation. To determine this global optimal window, we consider a weighted sum of the individual objective functions of each simulation (Supplementary Material Section 2). When applying the classification test to the area method, we must specify the time point at which the wound areas are measured and compared. We fix the comparison time to be half the time it takes the leading edges to touch each other in the first simulation which is a common choice in an experimental setting.

2.7 Implementation

The segmentation algorithm and the data analysis are implemented in MATLAB Version: 9.3.0.713579 (R2017b). The segmentation pipeline uses functions from Matlab's Image Processing Toolbox, the Grow Cut algorithm implementation found in `http://freesourcecode.net/matlabprojects/56832/growcut-image-segmentation-in-matlab` and the normality tests implemented by [31]. The agent-based model is implemented in NetLogo [32]. We do not apply the segmentation algorithm to the in silico images so the detection method does not affect the migration rate measurements.

3 Results

3.1 Exploration and validation of quantification method via in silico data

We first use the agent-based model to investigate how our quantification method is affected by cell motility and proliferation. Then, by applying the classification test, we investigate how well the method classifies cell populations with different motility and proliferation parameters in comparison with the other quantification methods.

3.1.1 Sensitivity analysis

We investigate how the windowed velocities are affected by the rates of cell migration and proliferation. We vary the motility and proliferation probabilities for fixed initial conditions. We decompose the parameter space of motility and proliferation probabilities $[0,1] \times [0, 0.01]$ into a regular 11×11 grid with 121 parameter

pairs (p_m, p_p). For each parameter combination, 150 simulations were performed and the windowed velocities were calculated. The optimal window was calculated with respect to all simulations for the same parameter combination. In Figure 4 A we present a contour plot of the mean windowed velocity which shows how, as the probabilities increase, the mean velocity increases. A similar trend is observed for the standard deviation (see Figure 4 B).

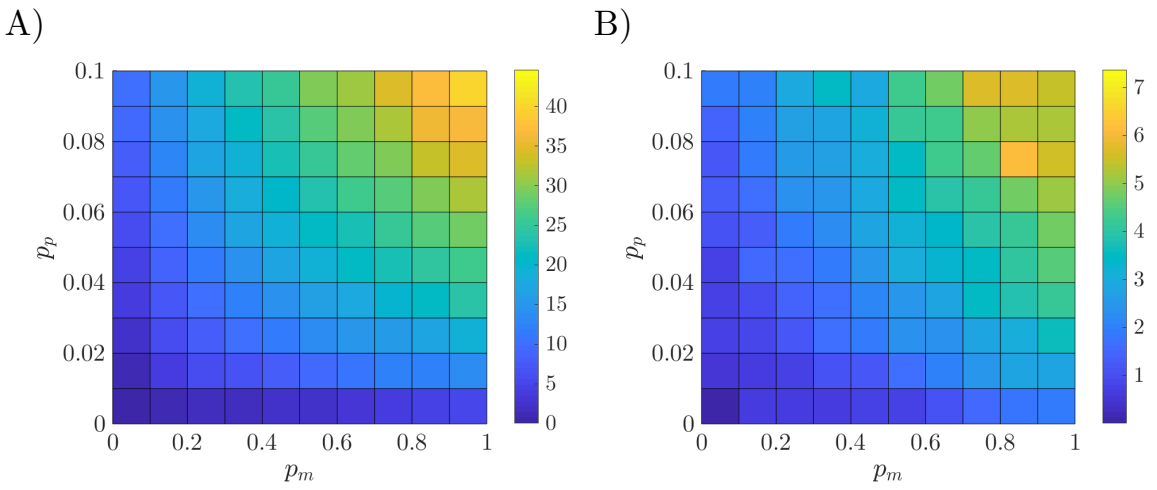

Figure 4: Sensitivity analysis of the agent-based model. We analyse the variability of the windowed velocities with respect to the proliferation and motility probabilities $(p_m, p_p) \in [0,1] \times [0, 0.1]$. In A) and B), we plot the mean and the standard deviation of windowed velocities of 150 simulations under each of these 121 parameter pairs.

3.1.2 Classification performance

We suppose that the focal parameter combination, $\hat{P} = (\hat{p}_m, \hat{p}_p)$, takes values in $\{0.1, 0.5, 0.9\} \times \{0.01, 0.05, 0.09\}$ in order to test the classification for small, medium and high values of cell motility and proliferation in our parameter space. We consider $n = 4$ simulations as the sample size for our test, so as to coincide with experimental settings in which four samples are typically used. We repeat the classification test 20 times to produce results that account for the stochasticity of the system.

In Figure 5, we plot the results of the mean behaviour of the classification tests when considering the K-S test and the three focal parameter combinations: $\hat{P} = (0.1, 0.01)$, $(0.5, 0.01)$ and $(0.9, 0.01)$. On each plot, the focal parameter combination is indicated by a red circle. At each position (p_m, p_p), we plot a circle whose colour corresponds to the percentage of times the migration measurements of that parameter pair are statistically significantly different to those for the focal parameters $\hat{P}$ with respect to the colourbar at the left of the plots. For parameter pairs different from the focal parameter, $(p_m, p_p) \neq \hat{P}$, if the percentage of times the migration measurements of that parameter pair are statistically significantly different to those for the focal parameters $\hat{P}$ is smaller than 100%, it indicates the presence of type II errors. For the focal parameter, $(p_m, p_p) = \hat{P}$, if this percentage is higher than 0% then it indicates the presence of type I errors. We can observe that for $\hat{P} = (0.1, 0.01)$, the classification is perfect: the K-S test indicated that the windowed velocities from simulations of parameter pairs different from the focal parameter, $(p_m, p_p) \neq \hat{P}$, are statistically significantly different to the windowed velocities from simulations of the focal parameter pair 100% of the time (Figure 5 A). For $\hat{P} = (0.5, 0.01)$, there are four parameter pairs different to the focal one for which the velocities were 80%, 85%, 85% and 95% times statistically significantly different to those for the focal parameter (Figure 5 B), and for $\hat{P} = (0.9, 0.01)$, the number of parameter pairs for which the percentage is not 100%, is increased (Figure 5 C). We observe that as the motility rate increases, the classification performance worsens.

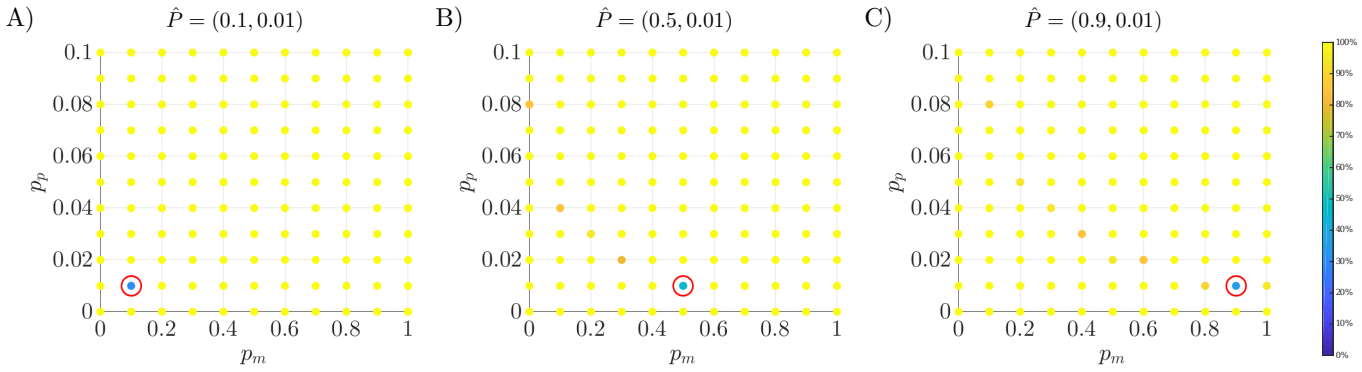

Figure 5: Plots of the mean behaviour of the classification tests for the velocity method. The classification tests are performed by considering a K-S test, a sample set of n=4 simulations and the focal parameters A) $\hat{P} = (0.1, 0.01)$, B) $\hat{P} = (0.5, 0.01)$, and C) $\hat{P} = (0.9, 0.01)$. In each plot at each parameter pair (p_m, p_p), the colour of the circle denotes the percentage of times the migration measurements of that parameter pair are statistically significantly different to those for the focal parameter $\hat{P}$. We indicate the focal parameter pair with a red circle. The plots illustrate how the classification performance of the method varies as the motility parameter varies. The method performs better when the motility parameter is small.

3.1.3 Comparison with standard migration quantification methods

We compare the classification performance of the velocity method with the closure rate and the area methods [4, 12]. As before, the focal parameter combination, $\hat{P}$, takes values in $\{0.1, 0.5, 0.9\} \times \{0.01, 0.05, 0.09\}$. We consider $n = 4$ simulations as the sample size and repeat the classification test 20 times.

In Figure 6, we plot the mean behaviour of the classification tests for the three quantification methods by applying the K-S test and the focal parameter combinations $\hat{P} = (0.1, 0.01)$, $(0.5, 0.01)$ and $(0.9, 0.01)$. We observe that for a focal parameter pair, the velocity method yields fewer incorrect classifications. We also observe that as the proliferation rate increases, the percentage number of incorrect classifications increases for the three methods.

The results of the classification tests for all other focal parameter combinations in $\{0.1, 0.5, 0.9\} \times \{0.01, 0.05, 0.09\}$ are presented in the Supplementary Material Section 3. Overall we observed that our method outperforms the closure rate and the area method. For all focal parameter combinations tested, the velocity method yielded a greater percentage of correct classifications. The performance of the area method was the worst while the performance of the closure rate method was intermediate between our method and the area method. The performance of all three methods declines as the motility and the proliferation rate of the focal parameters $\hat{P}$ increase.

3.2 Application of the quantification methods to in vitro data

Having tested the quantification methods on in silico data, we now use them to analyse experimental data. We first detect the position of the leading edges from the wound healing images taken during the course of the experiments. We then quantify the migration rates using the three quantification methods and analyse the statistical classification.

3.2.1 Image segmentation

After applying the segmentation algorithm, the front of the cell monolayer is detected for each time-lapse image. In Figure 1 we present the evolution of a representative scratch from each cell group (S1-S6).

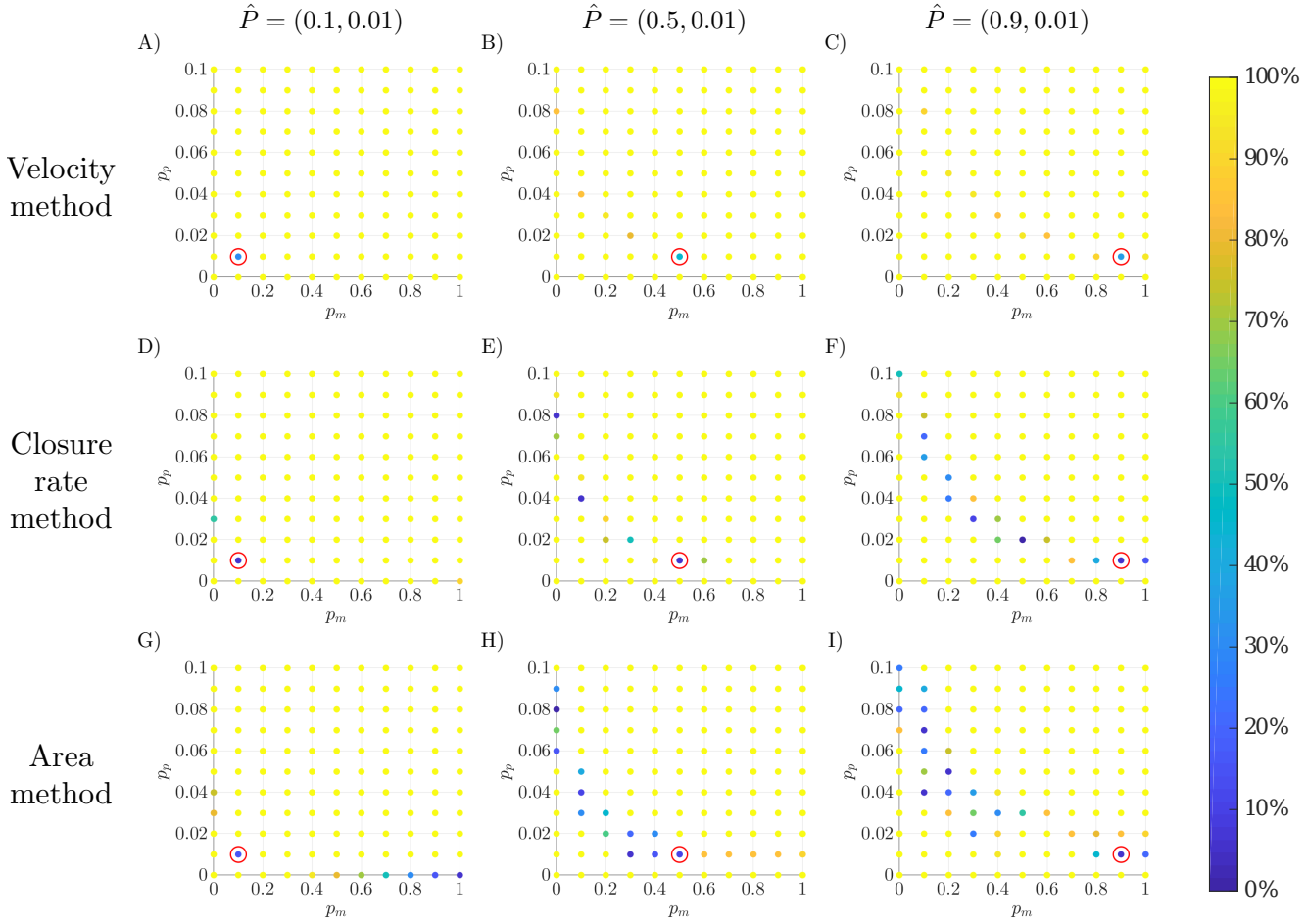

Figure 6: Series of plots showing how the performance of the three quantification methods changes as the motility rate of the focal parameters varies. In each plot, the colour of the circle at each parameter pair (p_m, p_p) indicates the percentage of times the migration measurements associated with the parameter pair are statistically significantly different from those associated with the focal parameters $\hat{P}$. The focal parameters $\hat{P}$ are indicated by a red circle. The results reveal that the velocity method yields a better statistical classification than the other methods. We note also the performance of all three methods declines as the motility rate of the focal parameters $\hat{P}$ increases.

3.2.2 Quantification method results

We quantify the migration velocity of scratch assays for the different cell types using the velocity method. We determine the global optimal window by calculating the objective function for the 24 scratch assays. We vary the window size w from 1 to 500μm with a step size of 1μm and use equation (7) to calculate the objective function $F(w)$. The objective function and the three fitness functions that contribute to its calculation are shown in the Supplementary Material Section 4. The maximum value is attained for a window size of 16μm. For a fixed window size ($w = 16\mu$m), we use a linear approximation to describe the evolution of the fronts and determine the 32 representative windowed velocities for each scratch assay and visualize their boxplots in Figure 7.

3.2.3 Statistical classification via the local quantification method

After grouping the velocities of scratch assays from the same cell type, the migration rate of each cell group is represented by 264 velocities. The boxplots associated with the velocity distributions for the six groups are shown in Figure 8 A. To determine how different the migration rate of cell group S1 is from the others, we

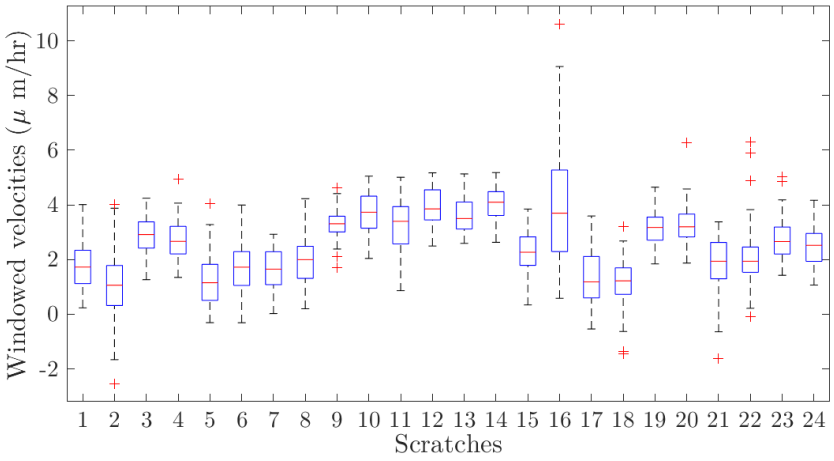

Figure 7: Boxplots of the windowed velocities with respect to the optimal window size 16 for each experimental scratch assay.

perform a K-S test to test the null hypothesis that the velocities from the two groups come from the same distribution. The null hypothesis was rejected for groups S2, S3 and S4 with statistical significance level of $p_{value} \leq 0.0001$. The null hypothesis was rejected for group S6 with statistical significance level of $p_{value} \leq 0.05$. For group S5, the null hypothesis was not rejected. We performed a t-test between S1 and each of the other groups to determine whether the mean difference is statistically significant. The mean difference between the velocities for cell groups S1 and S2, S3 and S4 is statistically significant at the 0.0001 level. There was statistical significance in the mean difference with respect to S6 at the 0.05 significance level. The statistical results for the K-S tests and t-tests are reported in Figure 8 A. The exact value of the p_{value} for each test is reported in the Supplementary Material Section 5.

3.2.4 Statistical comparison to standard migration quantification methods

We now compare the statistical results of our quantification method against those for the area and closure rate methods. In Figure 8 B) we plot the closure rates of each group and report the results from performing the K-S test and t-test between S1 and the other groups. S3 was the only group for which the null hypothesis of the K-S test and the t-test was rejected at the 0.05 significance level. When we performed the statistical tests for the percentage area measurements, no significant difference was found. In Section 5 of the Supplementary Material we include the results of the K-S and t-tests for the percentage wound area measurements.

4 Discussion and conclusions

In this work, we have introduced a new migration quantification method for scratch assays that characterizes the horizontal component of the front velocity of cell monolayers. The method involves three steps: (1) determination of an optimal window w^* with which to approximate the cell front by a function which is piecewise constant in segments of length w^*; (2) approximation of the interface with respect to the window size w^* at each time point; and (3) linear approximation of the evolution of the interface in each of these windows. In this way we characterize cell migration in the scratch assay by the slopes of a series of linear approximations to the interface evolution in these windows. The optimal window is chosen to be the one that best fits a constant velocity profile and for which the left and right front velocities can be consider to be samples of the same distribution.

By considering an agent-based model that mimics the scratch assay, we tested the ability of our quantification method to distinguish between cell lines with known cell motility and proliferation rates. As the motility and proliferation rates increased, the mean and variance of the windowed velocities increased. This was an expected behaviour since motility and proliferation promote the interface velocity and the variance of the

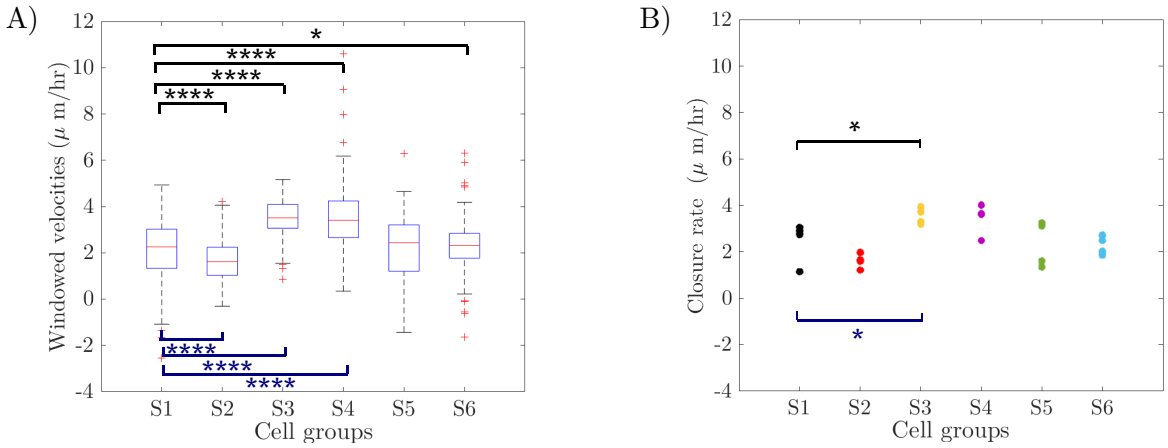

Figure 8: Statistical analysis of the experimental data using the velocity and the closure rate method. First, the migration measurements are grouped into the six different groups (S1-S6). The windowed velocities and the closure rates for the cell groups are plotted in A and B, respectively. Above the data, in black, we have reported the statistical significance results from performing a K-S test with respect to the S1 group. Below the data, we have done the same for the t-tests. Considering the windowed velocities, with respect to the K-S test and t-test, the null hypothesis was rejected testing group S1 against group S2, S3 and S4 at the 0.001 significance level. Performing the statistical tests with the closure rate measurements, the null hypothesis was rejected at the significance level of 0.05 between S1 and S3. The statistical significance level is decoded in the symbols: *:= $p_{value} \leq 0.05$, **:= $p_{value} \leq 0.01$, ***:= $p_{value} \leq 0.001$ and ****:= $p_{value} \leq 0.0001$

system increases as the motility and proliferation rates increase. By comparing our quantification method with two existing methods, we observed that our method outperforms both since it yielded a greater percentage of correct classifications than the other methods across a range of parameter values. We noticed that our method made significantly fewer statistical errors than the two other tested methods. Despite being widely used, the performance of the area method was the worst, while the performance of the closure rate method was intermediate between our method and the area method. The poor performance of the area method is due to the presence of irregular cell-free areas and to the indirect quantification of migration by a single time-point measurement. The poor performance of the closure rate method is also related to the irregularities in the data since the closure rate method is equivalent to quantifying the migration by the slope of the linear approximation to the evolution of mean position of the interface.

After showing that our quantification method performed better on in silico data, we then used it to analyse our experimental data set. We calculated an optimal window of 16 μm, which is of the same order as the mean cell diameter size, and then determined the corresponding windowed horizontal velocities. By performing two sample Kolmogorov-Smirnov (K-S) and unpaired two-sample t-tests, we identified a statistically significant difference between the S1 group and groups S2-S4. The K-S test also indicated statistically significant differences with respect to group S6. We used these two tests since we wanted to detect differences at the distribution level (through the K-S test) and at the mean level (through the t-test). The closure rate method only detected statistically significant differences between S1 and S3. The closure rate data are of poor quality: more samples or better quality ones are needed to analyse the migration rate with this method. The area method was unable to detect any statistically significant differences in the dataset. Even when we tried different time points, there was no significant difference. We observed that the S1 cell group also exhibited the highest levels of expression of target genes associated with malignancy and poor prognosis, when analysed by qRT-PCR techniques (data not shown) in agreement with the detected significant differences in migration.

There are several ways in which our study can be extended. The cell monolayer front evolution can be fitted to a Richards function, a non-symmetrical sigmoid function, which accounts for an initial phase during which the cells react to the presence of the wound, as in [11]. The statistical performance of our quantification

method can be further validated on publicly available wound healing experiment data sets such as those in [34], which provide sets of assays and replicates under different experimental conditions. The framework can also be extended to consider the evolution of the full velocity field across the full monolayer like the Cell Image Velocimetry (CIV) [36]. The challenge in doing this extension would be to determine which are the measurements to which we are going to apply statistical tests to detect significant differences in migration rates.

Data accessibility

The source code and the implementation of the algorithm as a GUI along with an example dataset and user instructions, are available in `https://bitbucket.org/anavictoria-ponce/local_migration_quantification_scratch_assays/src/master/`. The datasets are available in `https://ganymed.math.uni-heidelberg.de/~victoria/publications.shtml`.

Authors' contributions

TA, AM and SB designed and coordinated the study. AVPB developed the agent-based model and performed the processing and analysis of the data. SB and AVPB designed and developed the image processing pipeline. AM designed the experiments, while ES and JA performed them. HMB, PKM, TC and TA contributed to the analysis and interpretation of results. AVPB wrote the paper, on which all other authors commented and made editions. All authors gave final approval for publication.

Competing interests

The authors have no competing interests.

Funding

This work was supported by the Heidelberg Graduate School of Mathematical and Computational Methods for the Sciences [DFG grant GSC 220 in the German Universities Excellence Initiative to AVPB]; Mathematics for Industry Network [COST Action TD1409 short-term scientific missions grant to AVPB]; Consejo Nacional de Ciencia y Tecnología [411678 to JA]; Ministerio de Ciencia e Innovación [TIN2015-66951-C2-1-R and SGR 1742 to SB, SAF2017-89989-R to AM]; Red de Investigación Renal REDinREN [12/0021/0013 to AM]; the CERCA Programme of the Generalitat de Catalunya to TA; Ministerio de Economía y Competitividad [MTM2015-71509-C2-1-R and MDM-2014-0445 to TA] and Agència de Gestió de Ajuts Universitaris i Recerca [2014SGR1307 to TA].

Acknowledgements

AVPB would like to thank Isabel Serra Mochales, Matthew Simpson and Andreas Spitz for helpful discussions. We would like to thank Guillem Perez for being the initial promoter of this collaboration.

Footnotes

Electronic supplementary material is available online.

References

[1] Peter Friedl and Darren Gilmour. Collective cell migration in morphogenesis, regeneration and cancer. *Nature reviews Molecular cell biology*, 10(7):445, 2009.

[2] Li Li, Yong He, Min Zhao, and Jianxin Jiang. Collective cell migration: Implications for wound healing and cancer invasion. *Burns & trauma*, 1(1):21, 2013.

[3] Nina Kramer, Angelika Walzl, Christine Unger, Margit Rosner, Georg Krupitza, Markus Hengstschläger, and Helmut Dolznig. In vitro cell migration and invasion assays. *Mutation Research/Reviews in Mutation Research*, 752(1):10–24, 2013.

[4] Ayman Grada, Marta Otero-Vinas, Francisco Prieto-Castrillo, Zaidal Obagi, and Vincent Falanga. Research techniques made simple: Analysis of collective cell migration using the wound healing assay. *Journal of Investigative Dermatology*, 137(2):e11–e16, 2017.

[5] Chun-Chi Liang, Ann Y Park, and Jun-Lin Guan. In vitro scratch assay: a convenient and inexpensive method for analysis of cell migration in vitro. *Nature protocols*, 2(2):329, 2007.

[6] Kaylene J Simpson, Laura M Selfors, James Bui, Angela Reynolds, Devin Leake, Anastasia Khvorova, and Joan S Brugge. Identification of genes that regulate epithelial cell migration using an sirna screening approach. *Nature cell biology*, 10(9):1027, 2008.

[7] MNM Walter, Karina T Wright, HR Fuller, Sheila MacNeil, and W Eustace B Johnson. Mesenchymal stem cell-conditioned medium accelerates skin wound healing: an in vitro study of fibroblast and keratinocyte scratch assays. *Experimental cell research*, 316(7):1271–1281, 2010.

[8] Christine Decaestecker, Olivier Debeir, Philippe Van Ham, and Robert Kiss. Can anti-migratory drugs be screened in vitro? a review of 2d and 3d assays for the quantitative analysis of cell migration. *Medicinal research reviews*, 27(2):149–176, 2007.

[9] Steffen Nyegaard, Brian Christensen, and Jan Trige Rasmussen. An optimized method for accurate quantification of cell migration using human small intestine cells. *Metabolic Engineering Communications*, 3:76–83, 2016.

[10] Gebaeck. Tscratch: a novel and simple software tool for automated analysis of monolayer wound healing assays (vol 46, pg 265, 2009). *BioTechniques*, 46(6):383–383, 2009.

[11] Gil Topman, Orna Sharabani-Yosef, and Amit Gefen. A standardized objective method for continuously measuring the kinematics of cultures covering a mechanically damaged site. *Medical Engineering and Physics*, 34(2):225–232, 2012.

[12] Paola Masuzzo, Marleen Van Troys, Christophe Ampe, and Lennart Martens. Taking aim at moving targets in computational cell migration. *Trends in cell biology*, 26(2):88–110, 2016.

[13] Elia Ranzato, Simona Martinotti, and Bruno Burlando. Wound healing properties of jojoba liquid wax: an in vitro study. *Journal of ethnopharmacology*, 134(2):443–449, 2011.

[14] Heiko Büth, Pier Luigi Buttigieg, Raluca Ostafe, Maren Rehders, Stefanie R Dannenmann, Norbert Schaschke, Hans-Jürgen Stark, Petra Boukamp, and Klaudia Brix. Cathepsin b is essential for regeneration of scratch-wounded normal human epidermal keratinocytes. *European journal of cell biology*, 86(11-12):747–761, 2007.

[15] James EN Jonkman, Judith A Cathcart, Feng Xu, Miria E Bartolini, Jennifer E Amon, Katarzyna M Stevens, and Pina Colarusso. An introduction to the wound healing assay using live-cell microscopy. *Cell adhesion & migration*, 8(5):440–451, 2014.

[16] William J Ashby and Andries Zijlstra. Established and novel methods of interrogating two-dimensional cell migration. *Integrative Biology*, 4(11):1338–1350, 2012.

[17] Wang Jin, Esha T Shah, Catherine J Penington, Scott W McCue, Lisa K Chopin, and Matthew J Simpson. Reproducibility of scratch assays is affected by the initial degree of confluence: experiments, modelling and model selection. *Journal of theoretical biology*, 390:136–145, 2016.

[18] Wang Jin, Kai-Yin Lo, ShihEn Chou, Scott W. McCue, and Matthew J. Simpson. The role of initial geometry in experimental models of wound closing. *Chemical Engineering Science*, 179:221 – 226, 2018.

[19] Catalina Ruiz-Cañada, Ángel Bernabé-García, Sergio Liarte, Carmen Luisa Insausti, Diego Angosto, José María Moraleda, Gregorio Castellanos, and Francisco José Nicolás. Amniotic membrane stimulates cell migration by modulating transforming growth factor-β signaling. *Journal of tissue engineering and regenerative medicine*, 2017.

[20] Irina Gorshkova, Donghong He, Evgeny Berdyshev, Peter Usatuyk, Michael Burns, Satish Kalari, Yutong Zhao, Srikanth Pendyala, Joe GN Garcia, Nigel J Pyne, et al. Protein kinase c- regulates sphingosine 1-phosphate-mediated migration of human lung endothelial cells through activation of phospholipase d2, protein kinase c-ζ, and rac1. *Journal of Biological Chemistry*, 283(17):11794–11806, 2008.

[21] Stuart T Johnston, Joshua V Ross, Benjamin J Binder, DL Sean McElwain, Parvathi Haridas, and Matthew J Simpson. Quantifying the effect of experimental design choices for in vitro scratch assays. *Journal of theoretical biology*, 400:19–31, 2016.

[22] Stuart T Johnston, Matthew J Simpson, and DL Sean McElwain. How much information can be obtained from tracking the position of the leading edge in a scratch assay? *Journal of the Royal Society Interface*, 11(97):20140325, 2014.

[23] Matthew J Simpson, Kerry A Landman, and Barry D Hughes. Cell invasion with proliferation mechanisms motivated by time-lapse data. *Physica A: Statistical Mechanics and its Applications*, 389(18):3779–3790, 2010.

[24] Philip K Maini, DL Sean McElwain, and David I Leavesley. Traveling wave model to interpret a wound-healing cell migration assay for human peritoneal mesothelial cells. *Tissue engineering*, 10(3-4):475–482, 2004.

[25] Matthew J Simpson, Katrina K Treloar, Benjamin J Binder, Parvathi Haridas, Kerry J Manton, David I Leavesley, DL Sean McElwain, and Ruth E Baker. Quantifying the roles of cell motility and cell proliferation in a circular barrier assay. *Journal of the Royal Society Interface*, 10(82):20130007, 2013.

[26] Evgeniy Khain, Mark Katakowski, Scott Hopkins, Alexandra Szalad, Xuguang Zheng, Feng Jiang, and Michael Chopp. Collective behavior of brain tumor cells: the role of hypoxia. *Physical Review E*, 83(3):031920, 2011.

[27] Vladimir Vezhnevets and Vadim Konouchine. Growcut: Interactive multi-label nd image segmentation by cellular automata. In *proc. of Graphicon*, volume 1, pages 150–156. Citeseer, 2005.

[28] John Canny. A computational approach to edge detection. In *Readings in Computer Vision*, pages 184–203. Elsevier, 1987.

[29] GT Shrivakshan, C Chandrasekar, et al. A comparison of various edge detection techniques used in image processing. *IJCSI International Journal of Computer Science Issues*, 9(5):272–276, 2012.

[30] Richard M Heiberger and Burt Holland. *Statistical analysis and data display: an intermediate course with examples in R*. Springer, 2015.

[31] Metin Öner and İpek Deveci Kocakoç. Jmasm 49: A compilation of some popular goodness of fit tests for normal distribution: Their algorithms and matlab codes (matlab). *Journal of Modern Applied Statistical Methods*, 16(2):30, 2017.

[32] Seth Tisue and Uri Wilensky. Netlogo: A simple environment for modeling complexity. In *International conference on complex systems*, volume 21, pages 16–21. Boston, MA, 2004.

[33] Katrina K Treloar and Matthew J Simpson. Sensitivity of edge detection methods for quantifying cell migration assays. *PloS one*, 8(6):e67389, 2013.

[34] Assaf Zaritsky, Sari Natan, Doron Kaplan, Eshel Ben-Jacob, and Ilan Tsarfaty. Live time-lapse dataset of in vitro wound healing experiments. *GigaScience*, 4(1):8, 2015.

[35] Ronald J Adrian and Jerry Westerweel. *Particle image velocimetry*. Number 30. Cambridge University Press, 2011.

[36] Florian Milde, Davide Franco, Aldo Ferrari, Vartan Kurtcuoglu, Dimos Poulikakos, and Petros Koumoutsakos. Cell image velocimetry (civ): boosting the automated quantification of cell migration in wound healing assays. *Integrative Biology*, 4(11):1437–1447, 2012.